

*promoting access to White Rose research papers*



**Universities of Leeds, Sheffield and York**  
**<http://eprints.whiterose.ac.uk/>**

---

This is a paper published in **Convertech & e-Print**

White Rose Research Online URL for this paper:

<http://eprints.whiterose.ac.uk/43237/>

---

**Paper:**

Abbott, SJ, Kapur, N, Sleight, PA, Summers, JL and Thompson, HM (2011) *A review of the fluid mechanics of rigid roll coating systems*. *Convertech & e-Print*, 1 (2). 47 - 51 (5).

---

# A Review of the Fluid Mechanics of Rigid Roll Coating Systems

S.J. Abbott<sup>1</sup>, N. Kapur<sup>2</sup>, P.A. Sleight<sup>3</sup>, J.I. Summers<sup>2</sup> & H.M. Thompson<sup>2</sup>

<sup>1</sup>Consultant to Rheologic Ltd., UK; <sup>2</sup>Institute of Engineering Thermofluids, Surfaces & Interfaces (IESTI), School of Mechanical Engineering, University of Leeds, Leeds, UK; <sup>3</sup>School of Civil Engineering, University of Leeds, Leeds, UK.



H.M. Thompson@leeds.ac.uk

## 1. Introduction

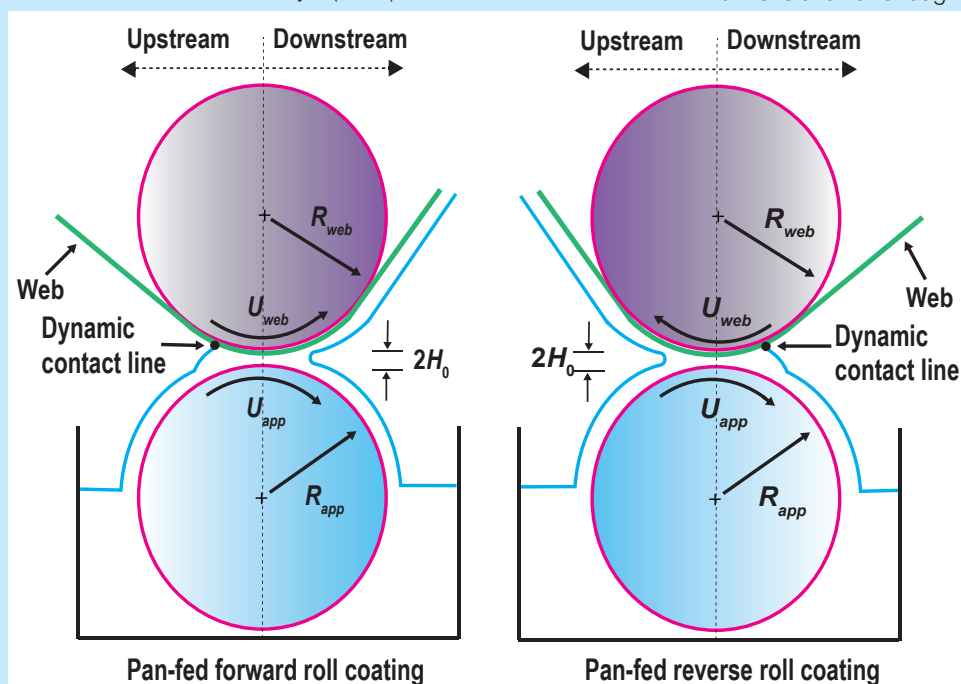
Roll coating systems are used to deposit liquid layers on continuous moving webs via the use of one or more rotating rolls. Such devices are used in applications such as the laying down of adhesives, decorative coatings on paper, metal and plastic, the precision coating of magnetic and optical media storage tapes, etc. This article provides a brief review of the fluid mechanical mechanisms that govern the behavior of rigid roll coating systems where the separation of the roll centers is bigger than  $(R_{app} + R_{web})$ . Such systems come in a variety of configurations and may involve a large number of rolls, any two of which will be operating in one of two modes shown in the following Figure: Forward roll coating—here the rolls contra-rotate so that their surfaces move in the same direction through the coating nip and Reverse roll coating—here the rolls co-rotate so that their surfaces move in the opposite direction through the coating nip. Typical operating conditions for each method are described in Coyle (1997).

Despite the wide variety of practical configurations, understanding the key features of these two modes of operation gives useful insight to any rigid roll coating system. When depositing a layer of liquid onto a moving web with a rigid roll coating system, the thickness and uniformity of the coating produced is determined by:

- The amount of liquid picked up by the applicator roll and transferred to the nip region.
- The minimum roll surface separation, or minimum gap, denoted as  $2H_0$ .
- The peripheral speeds of the web carrying roll,  $U_{web}$ , and the applicator roll,  $U_{app}$ , often expressed as Speed Ratio  $S = U_{web}/U_{app}$ .

Since the separation distance between the rolls compared to the length of rolls themselves is sufficiently large for axial flow to be deemed negligible provided roll run-out and roll eccentricity is minimized, flow can be considered to be two-dimensional far enough from either end of the roll pair.

The applicator roll picks up liquid, by the action of viscous lifting from a pan (or bath), transferring it to the nip region. Here it flows between the two roll surfaces where it splits at the downstream meniscus to form two coatings one of which is deposited on the web, the other remains attached to the applicator roll and returns to the coating pan. In some manufacturing situations it is necessary for the nip region to be fed directly from a large reservoir of liquid, see e.g. Thompson *et al* (2001).

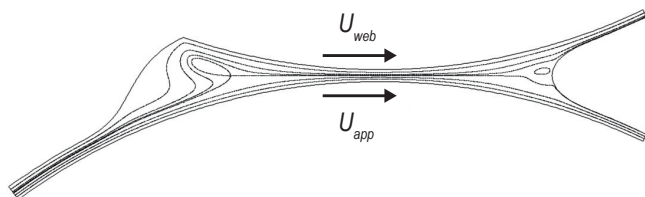


## 2. The Fluid Mechanics of Forward Roll Coating Systems

It is important to define the flooded and starved operating regimes. The coater is said to be operating with a flooded inlet if the applicator roll delivers a liquid layer with a thickness,  $H_{in}$ , greater than the minimum gap, that is  $H_{in} > 2H_0$ , and to be operating with a starved inlet if  $H_{in} < 2H_0$ .

### 2.1 The Inlet-Flooded (Classical) Operating Regime

This is the usual mode of operation and in the nip region the roll surfaces form a slowly converging/diverging channel such that the motion of the liquid between them is effectively one-dimensional. This feature is very important since it enables the flow there to be modeled accurately by using the famous Reynolds equation for pressure. The squeezing action of the converging flow on the inlet (upstream) side generates high pressures and the diverging nature of the flow in the downstream portion causes the pressure to fall below atmospheric near the downstream, film-split meniscus. Although the pressure distribution can be determined accurately from the one-dimensional Reynolds equation, the associated flow field is anything but one-dimensional near the menisci and a fuller analysis of it requires the use of computational methods, Summers *et al* (2004). The following figure is the result of actual computations and shows “streamlines” typical of inlet-flooded forward roll coating. A “streamline” can be thought of as the path traced out by a particle in a steady flow.



The main features of the flow are that:

1. It is effectively one-dimensional at and on either side of the minimum gap
2. Recirculating flow is evident near the downstream, film-split meniscus, the size of which is controlled by the Capillary number  $Ca = \mu U_{ave} / \sigma$ , where  $\mu$  is the viscosity,  $\sigma$  the surface tension, and  $U_{ave}$  the average roll speed,  $U_{ave} = (U_{app} + U_{web}) / 2$ , indeed forward roll coating flows for which  $Ca > 0.3$  tend to have no such recirculations present, Coyle (2007).
3. A rolling “bank” of liquid is present at the inlet.

The flow rate through the nip region of an inlet-flooded forward roll coater has been measured in many studies and

is usually expressed in terms of a non-dimensional flow rate,

$\lambda_{flooded}$ :

$$\lambda_{flooded} = \frac{Q_{flooded}}{H_0(U_{web} + U_{app})} \quad (1)$$

where  $Q_{flooded}$  is the flow rate through the nip region per unit length of the rolls (measured in  $m^2 s^{-1}$ ) and  $H_0$  is the semi-minimum gap width and  $\lambda_{flooded} \approx 1.34$ . The film split ratio is also needed to calculate the film thickness and the work of Gaskell *et al* (1998) predicts in the absence of gravity that:

$$H_{ratio} = \frac{H_{web}}{H_{app}} = \frac{S(S+3)}{(1+3S)} \quad (2)$$

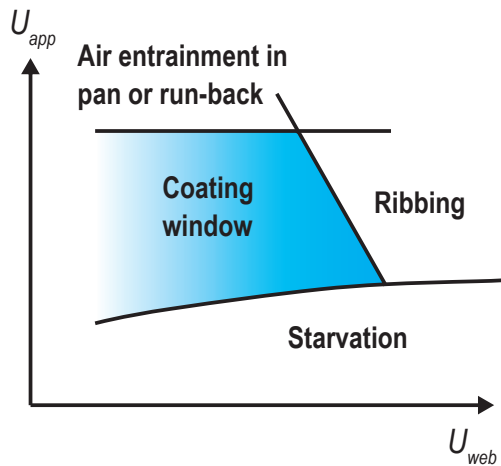
#### 2.1.1 Defects

Forward roll coating is particularly susceptible to “ribbing,” where the thickness of the coating varies across the web (in the axial direction of the rolls) giving rise to a sequence of regularly spaced stripes of unequal coat weight running in the direction of machine operation. It appears when the destabilizing effects of viscosity dominate over the stabilizing effects of surface tension at the downstream, film-split meniscus; the recent work by Zevallos *et al* (2005) discusses the effect of viscoelasticity on ribbing. The relative importance of viscous and surface tension effects is measured using the Capillary number, described by  $Ca = \mu U_{ave} / \sigma$ . In addition to a low Capillary number being required in order to avoid ribbing it is found that ribs can appear if too small a minimum gap setting is employed, Weinstein & Ruschak (2004). The dynamic wetting line is susceptible to air entrainment at sufficiently high coating speeds and the rolling bank can become unstable at high coating speeds. As shown above, inlet-flooded forward roll coating systems often contain recirculations which can trap bubbles and particulate contaminants, leading to defects such as “streaks.” Any non-uniformity in the inlet layer picked up by the applicator roll will result in a disturbance, e.g. due to perturbations to the process such as roll eccentricity or mechanical misalignment.

#### 2.1.2 Operating Window

The operability diagram for the inlet-flooded case (where liquid viscosities are usually quite high) is shown here, Coyle (1997). It shows that: (i) at high applicator roll speeds and relatively low web speeds, the process is limited either by excessive pick-up on the applicator roll ( $H_{in} \gg 2H_0$ ) which leads to “run-back” at the inlet or by air entrained as liquid is picked up from the coating pan; (ii) at high web speeds the process is severely limited by ribbing; (iii) the starvation limitation, when

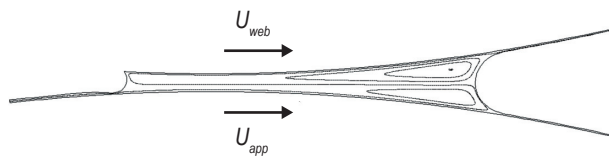
the applicator roll does not pick up sufficient liquid to flood the inlet, is only a problem for very low applicator roll speeds when high viscosity liquids are used.



Note that liquid viscosities used in industrial applications of ultra-starved coating (often called meniscus coating, Gaskell *et al* (1995)) are low (of the order of 0.001 Pa s) and  $U_{web}$  lies between 6 and 30 m min<sup>-1</sup>. In addition, corresponding capillary numbers which in this case are defined as  $Ca = \mu U_{app} / \sigma$  are small (of the order of 0.001). The transformation from inlet flooded to meniscus forward roll coating is described in Summers *et al* (2004).

### 2.2 The Inlet-Starved Operating Regime

In this case, the pressure distribution within the nip region is entirely below atmospheric, that is sub-ambient, with a profile that increases linearly from the upstream to the downstream meniscus. The streamlines are also very different as shown in the figure below:



The main features of the flow are that: (i) it is effectively two-dimensional with large regions of recirculating flow, extending throughout and occupying the majority of the flow field and (ii) liquid is transferred to the web by transfer jets which snake around the large eddies. In this regime neither the gap nor the web roll speed play any part in determining the flow rate as all the liquid in the inlet layer is transmitted through the nip region, which can be expressed in non-dimensional terms as, Gaskell *et al* (1995):

$$\lambda_{starved} = \frac{Q_{starved}}{U_{app}(2H_0)} = \frac{H_{in}}{H_0} \quad (3)$$

The only existing prediction for the film-split ratio is based on Landau & Levich (1942) and given as, Gaskell *et al* (1995):

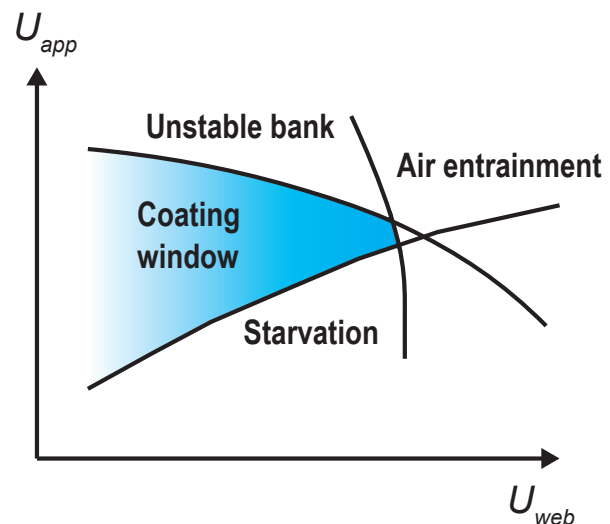
$$H_{ratio} = \frac{H_{web}}{H_{app}} = S^{2/3} \quad (4)$$

#### 2.2.1 Defects

As speed ratio  $S$  is increased from a stable operating condition the upstream free surface moves towards the nip and exhibits a local indentation or "necking" which leads to alternate wet and dry strips on the upper roll. This situation is remedied by reducing the web speed. If the applicator roll speed is reduced too far then it will not pick up sufficient liquid in order to feed the bead and the bead will break somewhere along its length followed by a disintegration along the bead—leaving a layer of liquid on the applicator roll only. Another common defect in the starved regime is the appearance of bubble lines in the coated web from the presence of bubbles in the bead. A bubble line is a region of localised, low coat weight and degassing within the liquid probably causes them.

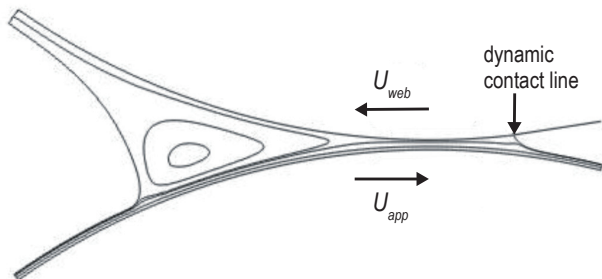
#### 2.2.2 Operating Window

The diagram below shows the operability limits for forward roll coating with low viscosity liquids, Coyle (1997), which is characteristic of the inlet-starved regime. It shows that: (i) if starvation is too great the bead will break or collapse; (ii) air entrainment can be a problem if the speed ratio  $S = U_{web}/U_{app}$  is too large; (iii) if, for a low viscosity liquid, the applicator speed is increased too far in order to pick up sufficient liquid to flood the inlet then the upstream bank may become unstable.



### 3. The Fluid Mechanics of Reverse Roll Coating Systems

As for the forward mode the flow is often assumed to be effectively one-dimensional through the minimum gap and several simple models of the flow in a reverse roll coater have emerged, based on lubrication theory, see e.g. Coyle (1997). However, in order to determine the precise nature of the flow, computational methods based on the Finite Element Method have been used, Thompson *et al* (2001). The figure below shows streamlines in an example of a pan-fed reverse roll coating system. Note that although in this case the web is wrapped around the upper, non-applicator roll, in practice the web is often wrapped around the applicator roll, in which case the other roll simply acts as a metering roll. The main features of the flow in the pan-fed case are: (i) recirculating flow near the upstream, film-split meniscus; (ii) a dynamic contact line where the downstream meniscus meets the web.



The coat thickness depends on gap and roll speed ratio  $S$ . It is effectively independent of viscosity. Most analyses of the flow have assumed that the inlet is flooded, i.e.  $H_{in} > 2H_0$ , and have been concerned with predicting how the final liquid thickness on the applicator roll,  $H_{app}$ , depends on the speed ratio  $S = U_{web}/U_{app}$ . They lead to:

$$H_{app} = KH_0(1 - S) \quad (5)$$

where  $K \approx 1.3$ . These models are only valid for cases where  $S \leq 1$ . Thompson *et al* (2001) derived a more accurate reverse film thickness prediction, for a reservoir-fed coating, by combining lubrication theory, pressure conditions at the free surfaces and conditions on the film thickness as a function of capillary number and the local curvature of the free surface. Coating quality also depends on  $S$ . At low reverse roll speed severe ribbing is encountered. At high reverse roll speed, the liquid meniscus is swept up into the nip and you get an unstable coating. The optimal operation is to obtain the roll speed ratio that is tuned for thickness and quality.

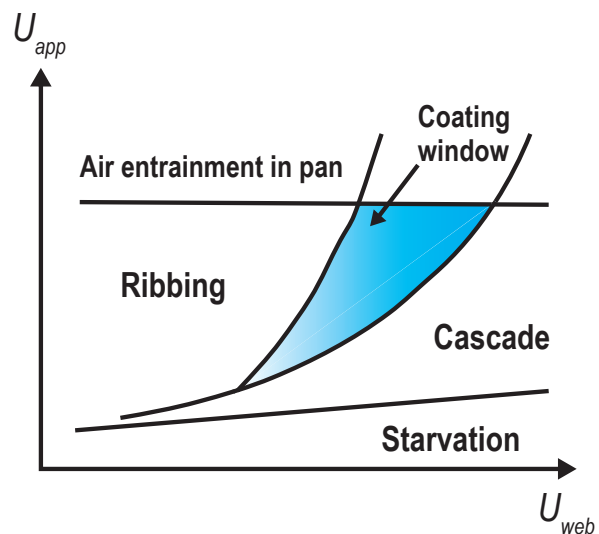
#### 3.1 Defects

The coating thickness in reverse roll coating is subject to “ribbing” and “cascade.” Ribbing—in reverse roll coating, the situation is more complicated because the de-stabilising effect of viscosity can be eliminated by increasing the web speed—is exactly what the industrialist wants to happen! This is a major reason why reverse roll coating is so useful because ribbing can be eliminated even when surface tension no longer has a stabilising influence. Cascade stems from the intrusion through the gap of the dynamic wetting line, when the wetting line periodically re-attaches to the web at the gap centre and is due to a speed ratio,  $S$ , that is too large. Coyle (1984) estimated that the critical speed ratio for the transition to cascade,  $S_{cascade}$ , could be expressed in terms of the Capillary number  $Ca$ :

$S_{cascade} \approx 0.43Ca^{-0.46}$  for gap widths in the range  $25 \leq H_0 \leq 250\text{m}$  and for  $0.2 \leq Ca \leq 4$ . As in the forward regime any non-uniformity in the inlet liquid layer picked up by the applicator roll will result in a disturbance of the inlet flow. There are several such types of disturbance, e.g. (i) ribs on the inlet layer, either inertially or viscosity driven, (ii) cross-bar type waviness as a consequence of uneven run-back or instability of the inlet layer and (iii) loss of stability at high applicator roll speeds.

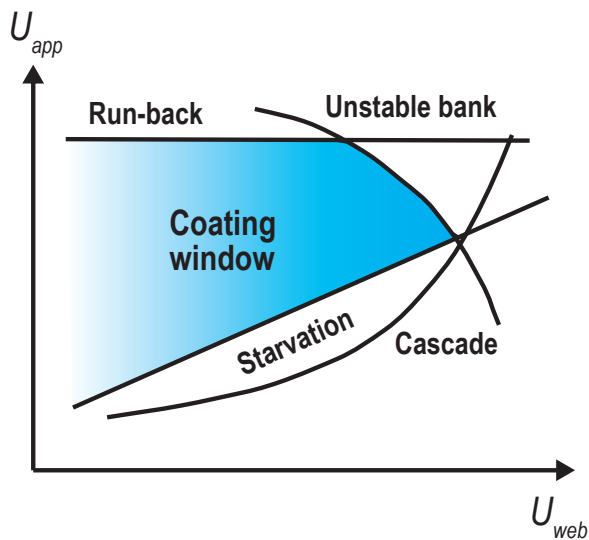
#### 3.2 Operating Window

Coyle (1997) gave operability diagrams for pan-fed reverse roll coating systems which are shown below. The left hand figure is an operability diagram for high viscosity liquids, while the right hand figure relates to low viscosity liquids. The diagram below shows that for high viscosity liquids: (i) ribbing may be experienced at relatively high applicator speeds,  $U_{app}$ , and (ii) ribbing can be eliminated by increasing the web speed  $U_{web}$ . However, there is a limit to the possible increase in  $U_{web}$  before the cascade instability appears. The applicator roll



speed  $U_{app}$  has to be large enough to avoid starvation (usually the case for high viscosity liquids) but air entrainment from the coating pan will become a problem if  $U_{app}$  is too large.

The diagram below shows that for low viscosity liquids: (i) severe starvation is a problem if  $U_{app}$  is too small, but if  $U_{app}$  is too large there may either be run-back on the inlet layer or an unstable upstream free surface; (ii) if  $U_{web}$  is too large then the cascade instability will occur.



#### 4. References

- [1] D.J. Coyle, Chapter 12a, *Liquid Film Coating*, Chapman & Hall, 1997.
- [2] H.M. Thompson, N. Kapur, P.H. Gaskell, J.L. Summers & S.J. Abbott, *Chem. Eng. Sci.*, Vol. 56, pp 4627-4641, 2001.
- [3] J.L. Summers, H.M. Thompson & P.H. Gaskell, *Theoret. Comput. Fluid Dynamics*, vol. 17, pp 189-212, 2004.
- [4] P.H. Gaskell, M.D. Savage & H.M. Thompson, *J. Fluid Mech.*, vol. 370, pp 221-247, 1998.
- [5] G.A. Zavallos, M.S. Carvahlo & M. Pasquali, *J. Non-Newtonian Fluid Mechanics*, Vol. 130 (2-3), pp 96-109, 2005.
- [6] S.J. Weinstein & K.J. Ruschak, *Ann. Rev. Fluid Mech.*, vol 36, 2004.
- [7] P.H. Gaskell, M.D. Savage, J.L. Summers & H.M. Thompson, *J. Fluid Mech.*, vol 298, pp 113-137, 1995.
- [8] L. Landau & B. Levich, *Acta Physicochim.* (USSR), vol. 17, pp 42-54, 1942.
- [9] D.J. Coyle, *PhD thesis*, University of Minnesota, 1984.

## FUJI Web Winder and Slitter Specialists

### Rotation Winder R

The latest automatic winder for high-functional films



#### FUJI products are suited to:

- High-functional film
- Industrial use film
- Packaging film
- Information recording film
- Agricultural film
- Flooring material and wallpaper
- Aluminum foil and cooking paper

**Our winders handle lithium-ion battery films, photovoltaic sheets, and FPD films**  
**Our slitters have produced results in various settings**

## FUJI TEKKO CO., LTD.

<http://www.fujitekko.co.jp/>



**Head Office & Katano Factory**  
 5-51-5 Hoshidakita, Katano City, Osaka, Japan 576-0017  
 TEL: +81-72-892-3611 FAX: +81-72-891-3455  
 E-mail: sd1@fujitekko.co.jp

**Tokyo Branch Office**  
 9F, Sakai Building, Kanda-sudacho 2-19-8, Chiyoda-ku, Tokyo, Japan 101-0041  
 TEL: +81-3-3258-1530 FAX: +81-3-3258-2775  
 E-mail: sd2@fujitekko.co.jp



Photovoltaic sealant sheet winder



Photovoltaic backsheet winder



Photovoltaic backsheet slitter



Lithium-ion battery separator film winder



Condensor film winder



Condensor film slitter